

CFD-BASED ANALYSIS OF THERMOCOUPLE MEASUREMENTS IN THE FIRE DECAY AND COOLING PHASES IN RELATION TO THE ADIABATIC SURFACE TEMPERATURE

Florian Put¹, Andrea Lucherini², Ruben Van Coile³, Bart Merci⁴

ABSTRACT

The definition of the thermal boundary conditions is usually the first step in a structural fire engineering calculation and is often represented by a single time-temperature curve, which should be referred to as an Adiabatic Surface Temperature. The validation of thermal boundary condition models is commonly performed based on data from large-scale fire experiments, in which thermocouple measurements provide temperature data, with focus on the post-flashover heating and fully-developed phases of a fire. The present study investigates whether thermocouple data obtained during the decay and cooling phases can serve as input for structural fire engineering calculations, and whether they can be used to compare against Adiabatic Surface Temperature models. To this purpose, a series of canonical FDS simulations is performed, representing the thermal boundary conditions that would be encountered in the fire decay and cooling phases, to study the impact of smoke and radiation on thermocouple measurements. The dynamically changing environment in which the thermocouples are situated during the decay and cooling phases (increased radiation due to dilution of the smoke) is shown to be incompatible with fixed values for the convective heat transfer coefficient and the effective emissivity, as used in the framework of the Adiabatic Surface Temperature.

Keywords: Thermocouple Measurements; CFD Simulations; Heat Transfer; Compartment Fires; Fire Safety; Adiabatic Surface Temperature

1 INTRODUCTION

Structural fire engineering (SFE) commonly encompasses a three-step procedure [1]. The initial step involves delineating the fire exposure scenario. Subsequently, thermal and mechanical analyses are conducted to assess the structure's response under a combination of thermal and mechanical loading [1].

The thermal boundary conditions arising from fire exposure can be expressed in various ways. In the most simplified case, they are represented with a single time-temperature curve. More complicated expressions of the thermal boundary conditions include heat fluxes of various natures, zone-models (either 1- or 2-zone

¹ MSc, PhD Researcher, Ghent University, Belgium

e-mail: Florian.Put@UGent.be, ORCID: <https://orcid.org/0000-0002-4522-9015>

² PhD, Senior Researcher, Slovenian National Building and Civil Engineering Institute (ZAG), Slovenia

e-mail: Andrea.Lucherini@zag.si, ORCID: <https://orcid.org/0000-0001-8738-1018>

³ PhD, Ghent University, Belgium

e-mail: Ruben.VanCoile@UGent.be, ORCID: <https://orcid.org/0000-0002-9715-6786>

⁴ Prof., Ghent University, Belgium

e-mail: Bart.Merci@UGent.be, ORCID: <https://orcid.org/0000-0002-2600-0098>

models) or results from Computational Fluid Dynamics (CFD) calculations [1]. When a single time-temperature curve is used, the implicit assumption is that the convective and radiative heat transfer can be replaced by a single temperature, usually associated with the gas phase, and the applied time-temperature curve represents what is commonly known as the *Adiabatic Surface Temperature* (AST) [2]. This concept relies on a single time-temperature curve, employing fixed values for the convective heat transfer coefficient and effective emissivity, to simplify the expression of the thermal boundary conditions [2].

Literature provides several models to define the thermal boundary conditions with a single time-temperature curve, such as the Eurocode Parametric Fire Curve [3], the BFD-curve [4] and one-zone models such as Ozone. The validation of such models was often based on data from large-scale experiments and mainly focused on the heating and fully-developed phases. Traditionally, the fire decay and subsequent cooling phases were not of interest and therefore neglected. Although the AST can be estimated using a plate thermometer (an idealized plate thermometer would measure the real AST [2]), plate thermometer data is scarce in literature as most large-scale fire experiments primarily use thermocouples to provide temperatures. If thermocouple data is to be used to validate models in the fire decay and cooling phase, a crucial step involves a discussion of the experimental data for temperatures as reported during those phases.

A fire generally consists of several phases (i.e., growth, fully-developed, decay and cooling phases), each with specific thermal boundary conditions [5]. Therefore, it can be expected that the temperatures recorded by thermocouples are also affected in different ways during the different stages of a fire [5]. In particular, the fire decay phase is characterised by a decreasing heat release rate (HRR) of the fire, leading to a reduction in the smoke production and an increased intake of cold air, diluting the smoke. Hence, the optical density of smoke decreases significantly as compared to the fully-developed phase [5]. The cooling phase is characterised by the absence of smoke. The smoke is replaced by cold air, continuously flowing into the compartment, once the fire extinguished, and cooling the structural elements inside [5].

This study focuses on the temperatures as measured by thermocouples, especially during the fire decay and cooling phases, and how they relate to the wide-spread concept of *Adiabatic Surface Temperature*. To this end, the theoretical background of the AST is revisited first. Subsequently, the outcomes of a series of canonical Fire Dynamics Simulator (FDS) calculations are leveraged, focusing on the influence of the smoke and radiation on thermocouple measurements, and their relationship to the AST.

2 ADIABATIC SURFACE TEMPERATURE

2.1 Theoretical background

The thermal boundary conditions of a surface exposed to fire can be characterized by the net heat flux to the surface, typically comprising conductive, convective, and radiative components. When addressing heat transfer between a solid surface and a gas, the conductive aspect is often considered negligible in comparison to the convective and radiative terms. Consequently, the net heat flux can be expressed as [2]:

$$\dot{q}_{tot}'' = \varepsilon (\dot{q}_{inc}'' - \sigma \cdot T_s^4) + h (T_g - T_s) \quad (1)$$

where

- \dot{q}_{tot}'' is the total (net) heat flux [W/m²],
- ε is the effective emissivity [-],
- \dot{q}_{inc}'' is the incoming radiative heat flux [W/m²],
- σ is Stefan-Boltzmann's constant [W/m²K⁴],
- h is the convective heat transfer coefficient [W/m²K],
- T_g is the gas temperature [K]
- T_s is the surface temperature [K].

Assuming that the incoming radiative heat flux \dot{q}_{inc}'' can be expressed as a function of the radiation temperature, T_r , equation (1) can be rewritten as [2]:

$$\dot{q}''_{tot} = \varepsilon \cdot \sigma (T_r^4 - T_s^4) + h (T_g - T_s) \quad (2)$$

The radiation temperature, T_r , is the temperature of a black-body emitter that causes the same incident radiative flux on the surface as q''_{inc} . As convection and radiation represent the dominant modes of heat transfer between elements (solids) and the gas phase during a fire, both equation (1) and equation (2) are generally applicable. The total net heat flux formulation of equation (1) and equation (2) has the drawback that it depends on two variables, q''_{inc} (equation (1)) or T_r (equation (2)) and T_g . As a workaround, an adiabatic surface can be considered, which by definition does not absorb any heat due to its thermal equilibrium as it is adiabatic and has a negligible mass [2]. Therefore, the net heat flux to such a surface has to be zero (first law of thermodynamics [6]) and steady-state conditions are implicitly assumed. The heat balance of equation (2) can be rewritten as in equation (3), assuming that the effective emissivity, ε_{AST} , and convective heat transfer coefficient, h_{AST} , are known or have been decided upon.

$$\varepsilon_{AST} \cdot \sigma (T_r^4 - T_{AST}^4) + h_{AST} (T_g - T_{AST}) = 0 \quad (3)$$

By combining the heat transfer equations outlined in equation (2) and equation (3), the total heat transfer can be computed as follows [2]:

$$\dot{q}''_{tot} = \varepsilon_{AST} \cdot \sigma (T_{AST}^4 - T_s^4) + h_{AST} (T_{AST} - T_s) \quad (4)$$

The AST, thus, represents a weighted average of T_r and T_g . The weighting factor is contingent on the ratio $h_{AST}/\varepsilon_{AST}$. As the AST employs a single temperature to express the thermal boundary conditions, the concept is highly appealing for utilization as input in structural fire engineering calculations. The same procedure can theoretically be always applied, across the entire post-flashover fire scenario, encompassing the decay and cooling phases. Yet, special attention with respect to the values of the convective heat transfer coefficient and effective emissivity (and radiation in general) is needed, as explained below in section 2.2.

2.2 Comments on the Adiabatic Surface Temperature

Although the AST is a useful concept that simplifies the thermal boundary conditions of structural elements by representing the total heat transfer by a single temperature, it also has drawbacks regarding applicability. It is a purely mathematical concept, based on the idealized concept of an adiabatic surface, which is usually simplified in an ideal ‘plate thermometer’ and the assumptions made do not reflect the conditions during real fire exposure.

The AST is generally based on fixed values for the convective heat transfer coefficient (e.g., 25 W/m²K for standard fire exposure and 35 W/m²K for natural fire exposure according to EN 1991-1-2 [3]) and the effective emissivity of the emitting and receiving surfaces. These values have been determined for the post-flashover fully-developed phase, but do not consider the changes in thermal boundary conditions once the fire advances into subsequent phases such as the fire decay phase and the cooling phase. Indeed, when the HRR of a fire decreases, the compartment flows induced by the fire also decrease. Hence, the convective heat transfer coefficient should decrease. When the fire has completely extinguished, during the cooling phase, the value should reduce even further as the external source for flows completely disappears and compartment elements cool by natural convection. Therefore, it is incorrect to use experimental data from plate thermometers during the fire decay and cooling phases directly in a calculation with a fixed convective heat transfer coefficient. As the AST is a purely mathematical concept, however, the measured plate thermometer temperatures can be recalculated to fit calculations with a fixed convective heat transfer coefficient, provided that the conditions during the fire (and thus also the real convective heat transfer coefficient) are known.

2.3 Implementation in FDS

FDS is a CFD tool developed by NIST, designed specifically to perform fire simulations. It is a large-eddy simulation code, solving a form of the Navier-Stokes equations for low speed flows, and focusses on the modelling of smoke and heat transfer phenomena [7]. It is widely used in fire safety engineering to predict

the behaviour of fire when experiments are not feasible or economical, aiding for example fire risk assessment and evacuation plans.

FDS incorporates two distinct devices to record the AST during a simulation, associated with the output quantities '*Adiabatic Surface Temperature*' and '*Adiabatic Surface Temperature Gas*' [7]. The difference between the two output quantities is subtle, yet of high importance as the results between the two formulations are different.

When a device with the output quantity '*Adiabatic Surface Temperature*' is employed, it should be positioned on the interface between a gas and a solid. To estimate the total net heat flux, with regards to convection, FDS calculates the convective heat transfer coefficient based on the velocity of the flow over the surface at the position where the device is located and the respective temperatures of the gas and surface at that point. In addition, with regards to radiation, FDS assumes that the effective emissivity of the solid also applies to the AST calculation [7]. As a result, the convective heat transfer coefficient is not fixed during the simulation. Instead, it varies throughout the simulation. The calculation of the AST is thus based on continuously changing parameters and to apply the AST in calculations, the values of these parameters should be tracked. This method represents what a plate thermometer would measure in a real experiment.

When a device with the output quantity '*Adiabatic Surface Temperature Gas*' is used, the requirement of positioning it at the interface between a gas and a solid cancels. The device can be freely positioned within the gas phase, but a fixed value for the convective heat transfer coefficient and effective emissivity must be provided [7]. Values for the convective heat transfer coefficient and effective emissivity are chosen and kept constant during the entire fire scenario, even though this may not align with the values during a real fire. This approach resembles the way the concept of AST is typically applied in SFE calculations.

3 NUMERICAL SIMULATIONS SET-UP

To investigate the impact of environmental radiation and smoke on thermocouple measurements during a fire in relation to the AST, a basic setup has been developed in Fire Dynamics Simulator (FDS, version 6.8.0) [7]. The setup consists of a 1 m by 1 m by 1 m cubical box, with small holes of 5 cm by 5 cm in the corners of the floor and ceiling to allow for flow into and out of the cube. The walls are modelled as adiabatic surfaces. Temperatures are recorded by a thermocouple tree, which is positioned in the middle of the cube, as indicated in Figure 1. Thermocouples (output quantity 'THERMOCOUPLE') have been positioned on the tree with 10 cm intervals, starting at 10 cm from the ceiling and extending to 10 cm from the floor. Additionally, temperature devices (output quantity 'TEMPERATURE') have been added at the same locations to record 'real' gas temperatures. In the first part of the analysis, also Adiabatic Surface Temperatures were recorded. Two devices with the output quantity '*Adiabatic Surface Temperature*' were positioned in the middle of the floor and ceiling. Similarly, two devices with output quantity '*Adiabatic Surface Temperature Gas*' were positioned directly in front of the floor and ceiling, with fixed convection coefficient of 35 W/m²K (as specified in [3] for natural fire exposure) and a fixed effective emissivity of 0.9. The mesh cell size was 5 cm, which does not allow for detailed modelling of the inflow and outflow of air and smoke into/from the compartment, but that is not essential for the study at hand as the focus is on thermocouple measurements. A sensitivity analysis has been performed to confirm this and is presented in section 4.4.

The analysis consists of three scenarios, of which the details are presented in Table 1, with varying radiation attenuation coefficient and soot mass fraction in the smoke. To this purpose, the cube is filled with a hot smoke, with different levels of smoke optical thickness and temperature. The optical thickness of the smoke is determined by 2 factors, being the soot mass fraction and the mass extinction coefficient, K_m . The soot mass fraction represents the mass of soot per unit mass of smoke and thus governs the smoke density, while the mass extinction coefficient indicates the attenuation of radiation by smoke per unit of smoke density. In other words, multiplication of the smoke density and mass extinction coefficient, K_m , results in the radiation extinction coefficient, K . Given that K , the incident monochromatic intensity, I_0 , and the travel distance of radiation through the smoke, L , are known, the transmitted intensity, I , of monochromatic radiation through smoke is given by equation (5) [8].

$$I = I_0 e^{-KL} \quad (5)$$

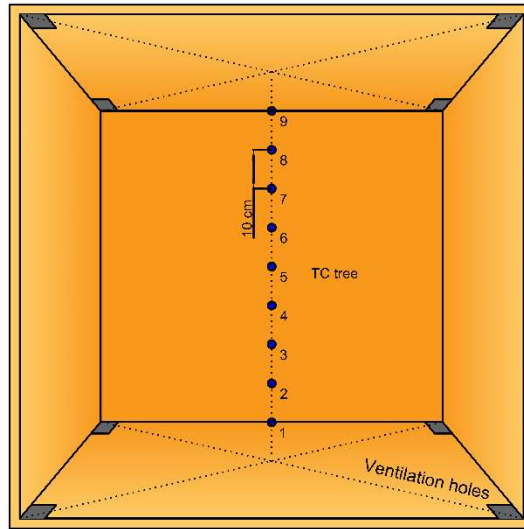


Figure 1. Box geometry used in FDS simulations.

Scenarios 1 and 2 represent the onset of the decay phase, immediately after the fully-developed phase, with Scenario 1 having an optically very thick smoke and Scenario 2 having an optically less thick smoke. Scenario 3 represents the onset of the pure cooling phase, immediately after the decay phase has ended. As mentioned before, smoke has left the compartment during this phase, but the linings and structural elements inside are still hot as, due to their thermal inertia, they cool down slower than the compartment gases. Parameters that are not explicitly provided in Table 1 are left according to the FDS default values.

Table 1. Description of decay and cooling phase scenarios.

Scenario	T_{ceiling} [°C]	T_{floor} [°C]	T_{smoke} [°C]	Mass Extinction Coefficient, K_m [m ² /kg]	Soot Mass Fraction [-]
1. Onset decay	1000	400	1000	20000	0.1
2. Onset decay	1000	400	750	500	0.005
3. Onset cooling	1000	400	No smoke		

4 RESULTS

4.1 Scenario 1

Scenario 1 marks the transition from a fully-developed phase with an optically very thick smoke to the fire decay phase, which is characterised by a diminishing HRR of the fire. The initial conditions of FDS are such that the thermocouples are initially at ambient temperature (i.e., 20°C), whereas the smoke inside the compartment is initially at elevated temperature (1000°C in this case, as specified in Table 1).

As the smoke is initially hot, buoyancy in the smoke is evident from the onset of the simulation. The hot smoke leaves the compartment immediately after the simulation has started through the holes in the ceiling, while cold air enters the compartment through the holes in the floor. The thermocouples, which are initially cold, increase in temperature immediately after the onset of the simulation as they are surrounded by the hot smoke. Both effects are observed in Figure 2b and Figure 2a respectively, while the large negative values at the onset of the calculation in Figure 2c are caused by the initial conditions in FDS.

The thermocouple measurements at different heights over time are a complex interaction between location (more specifically the distance to radiating surfaces), smoke optical thickness and the corresponding

attenuation of radiation, and the smoke temperature. Initially, the smoke has a very high optical thickness (Figure 3a). Radiation from the ceiling and floor cannot affect the thermocouple temperature as radiation is absorbed by the smoke, which emits radiation based on its own temperature. Once smoke flows out of the box and fresh air enters, the optical thickness in the lower regions is reduced. The onset of this phenomenon can be observed in Figure 3b, while the reduction is more visible in Figure 3c. Thermocouples near the floor exchange heat with both the smoke layer on top and the floor. Radiation from the ceiling is still blocked as the optical thickness of the smoke is still high in the upper regions of the compartment. Given that the smoke clears faster at the bottom, the bottom thermocouples tend to a stabilized temperature faster.

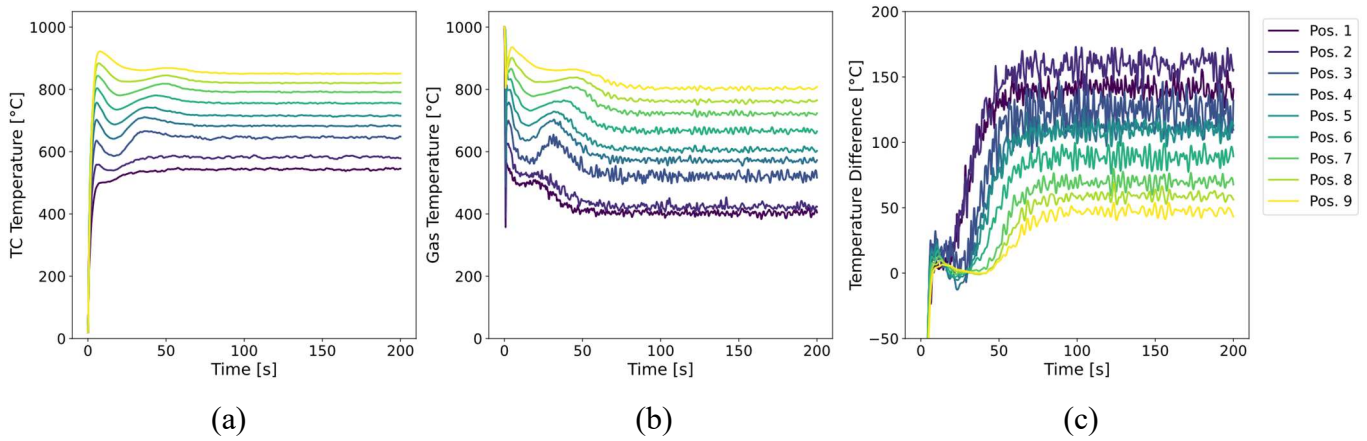


Figure 2. Temperatures measured by (a) thermocouples (TC): T_{TC} and (b) temperature devices (TD): T_g , and (c) the difference $T_{TC} - T_g$ in Scenario 1. Pos. 1 to 9 as specified in Figure 1.

Once all the smoke has exited the compartment (see Figure 3d), radiation from the ceiling affects the thermocouple temperatures as air is transparent. The air inside the compartment stratifies due to the presence of the floor and ceiling, which are at different temperatures. There still is a flow inside the compartment as the hot air leaves the compartment due to buoyancy and fresh air enters, but as the optical thickness remains constant (air remains transparent), this flow no longer affects the thermocouple temperatures. At this point, the system has reached steady state, starting from around 90s after the onset of the simulation.

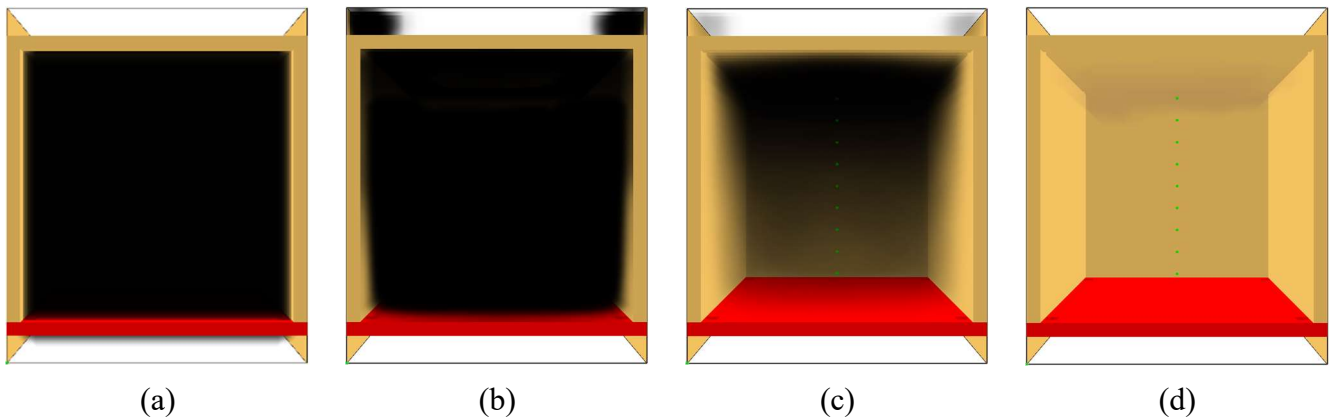


Figure 3. Visualization of smoke density in Scenario 1 at (a) 0s , (b) 20s, (c) 50s, and (d) 90s.

Once the smoke has left the compartment and a steady state has been reached, it can be observed that the temperature difference between the thermocouples temperature and the local gas temperature is greater near the floor, even though the view factor from the hottest surface (the ceiling) decreases with distance. Radiative heat transfer depends on both geometry (expressed through the view factor) and the difference in

the fourth power in temperatures. Because of the stratification of air within the compartment, the temperature difference between the ceiling and a thermocouple is more pronounced near the floor, leading to increased radiative heat transfer. This phenomenon outweighs the change in view factor caused by shifting position within the compartment. Consequently, the difference between gas temperature and thermocouple readings increases with distance from the ceiling. Similarly, the AST is higher at the floor than at the ceiling, as depicted in Figure 4. However, positions 1 and 2 show an exception where the temperature difference between thermocouples and gas temperature is larger at position 2 than at position 1 (see Figure 2c). This discrepancy is due to the intake of fresh air, resulting in a relatively small difference in gas temperature between the positions, as evident in Figure 2b. Since the view factor remains constant, the thermocouple at position 2 receives more radiation, leading to a greater temperature disparity.

Under the conditions of Scenario 1, the difference between the output quantities '*Adiabatic Surface Temperature*' and '*Adiabatic Surface Temperature Gas*' is examined. This disparity practically reflects the difference between experimental measurement and use of the AST as parameter in SFE calculations, as discussed in section 2. Figure 4 illustrates how the recorded AST from both outputs diverges over time in relation to the optical thickness of the smoke, represented by the soot density in the air. It is notable that under high soot density, the two AST output quantities almost coincide. However, as the optical thickness of the smoke decreases, disparities emerge between the two formulations. In particular, the '*Adiabatic Surface Temperature Gas*' output exhibits higher values than the '*Adiabatic Surface Temperature*' output near the ceiling, but lower near the floor.

Considering that the emissivity remains constant in both cases (0.9 as specified for the output quantity '*Adiabatic Surface Temperature Gas*', consistent with the default value used in FDS), the observed differences arise from variations in the convective heat transfer. At the ceiling, the overestimation of the convective heat transfer coefficient results in an increase of the AST. Consider the AST to be measured by an infinitesimally small ideal plate thermometer, placed on the ceiling. This device can be conceived as a very thin plate (such that it does not have any heat capacity) of which the backside is perfectly insulated, representing an adiabatic surface. Due to the perfectly insulating layer, the device cannot exchange heat with the surface it is positioned on, but it can exchange heat with the other surfaces in the compartment (only the floor in the considered geometry).

The ideal plate thermometer solely exchanges heat with the floor and not with the ceiling. Hence, it maintains a lower temperature compared to the surrounding gas, which is transparent and does not engage in radiation exchange. Consequently, an overestimated convective heat transfer coefficient results in an increase in adiabatic surface temperature. Conversely, at the floor, an overestimation of the convection coefficient induces a temperature decrease. Here, the ideal plate thermometer solely interacts with the ceiling, and thus maintains a higher temperature relative to the surrounding gas. Consequently, overestimated convection results in cooling of an adiabatic surface and thus also a lower adiabatic surface temperature. Quantitatively, this difference at steady state manifests as approximately 19°C at the ceiling, representing a discrepancy of roughly 2.6%, whereas at the floor, the values are respectively 47°C and 6.0%. As a reference for these values, the temperature increase from ambient (20°C) of the real AST is used (i.e., with varying convective heat transfer coefficient, denoted as AST Ceiling and AST Floor in the legend of Figure 4).

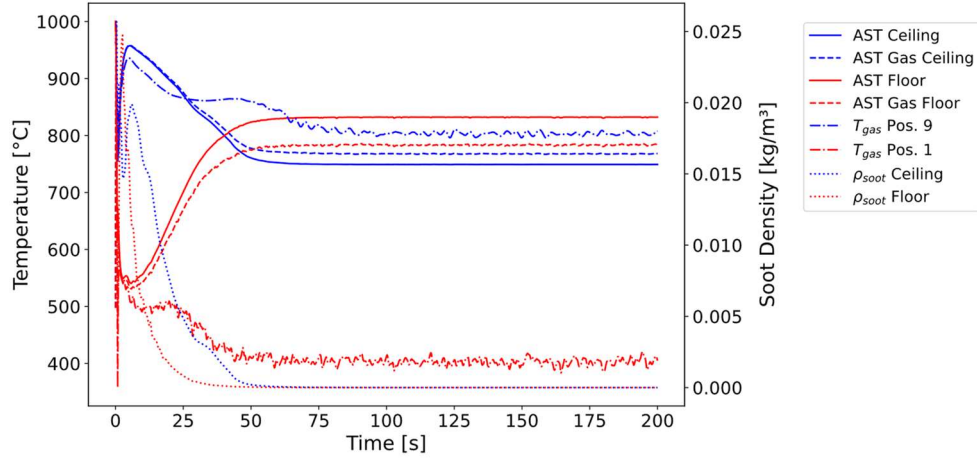


Figure 4. Adiabatic surface temperatures and soot densities in the middle of the ceiling and floor in Scenario 1.

4.2 Scenario 2

Similar to Scenario 1, Scenario 2 also depicts the transition from the fully-developed phase to the decay phase. However, the initial optical thickness of the smoke is significantly lower compared to Scenario 1, while the initial smoke temperature is decreased to 750°C (see Figure 5b). The thermocouples are initially at 20°C, as depicted in Figure 5a.

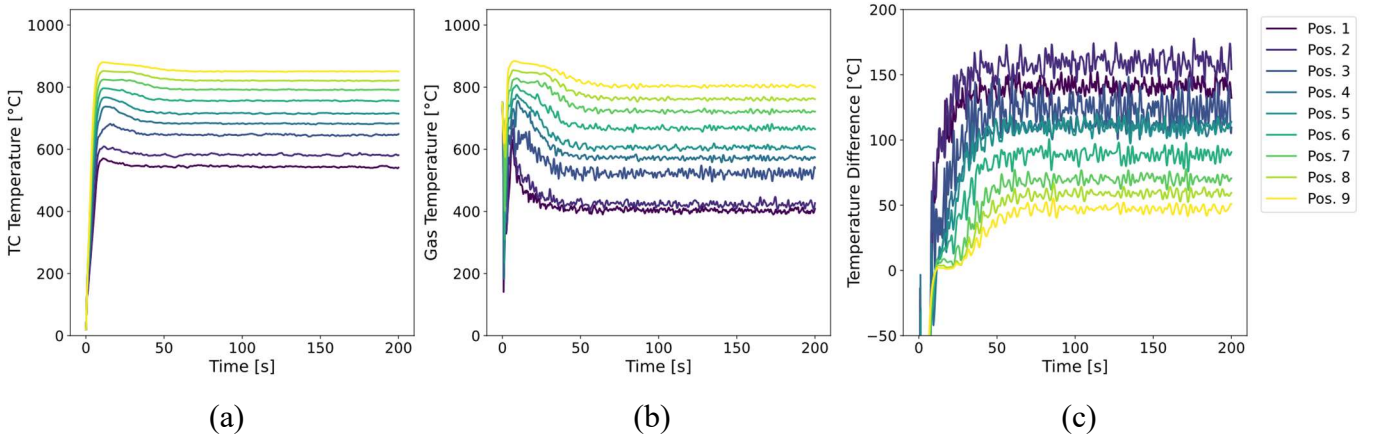


Figure 5. Temperatures measured by (a) thermocouples (TC): T_{TC} and (b) temperature devices (TD): T_g , and (c) the difference $T_{TC} - T_g$ in Scenario 2. Pos. 1 to 9 as specified in Figure 1.

At the beginning of the simulation, the same phenomena as in Scenario 1 take place. Due to its elevated temperature, buoyancy in the smoke is evident from the beginning. The smoke leaves the compartment through the holes in the ceiling, while fresh air enters through the holes in the bottom, as can be observed from the transition in Figure 6. Simultaneously, the thermocouples heat up as they are surrounded by hot smoke (see Figure 5a). The overall behaviour is similar to Scenario 1, but steady state is reached more quickly (after approximately 50s compared to 80s in Scenario 1) and the influence of radiation is observed sooner (after about 10s instead of 25s). According to equation (5), a lower extinction coefficient, K , results in a lower attenuation of radiation by smoke. The extinction coefficient, K , is determined by multiplying the mass extinction coefficient, K_m , by the smoke density, which is influenced by the soot mass fraction. As both parameters were initially lower compared to Scenario 1, K was also lower, leading to a head start in the decline in the attenuation of radiation by smoke until it becomes negligible.

Once the smoke has completely left the compartment, both the thermocouple and gas temperatures tend to the same steady-state situation as in Scenario 1. The difference between thermocouple and gas temperatures increases with increasing distance from the ceiling. Similar to Scenario 1, the stratification in the air,

induced by the temperature difference between the floor and ceiling, leads to variations in the temperature difference between thermocouples and the radiating surfaces. These variations have a bigger effect than the changes in view factor with position, resulting in a higher difference in temperature between thermocouple and gas as the distance from the ceiling increases.

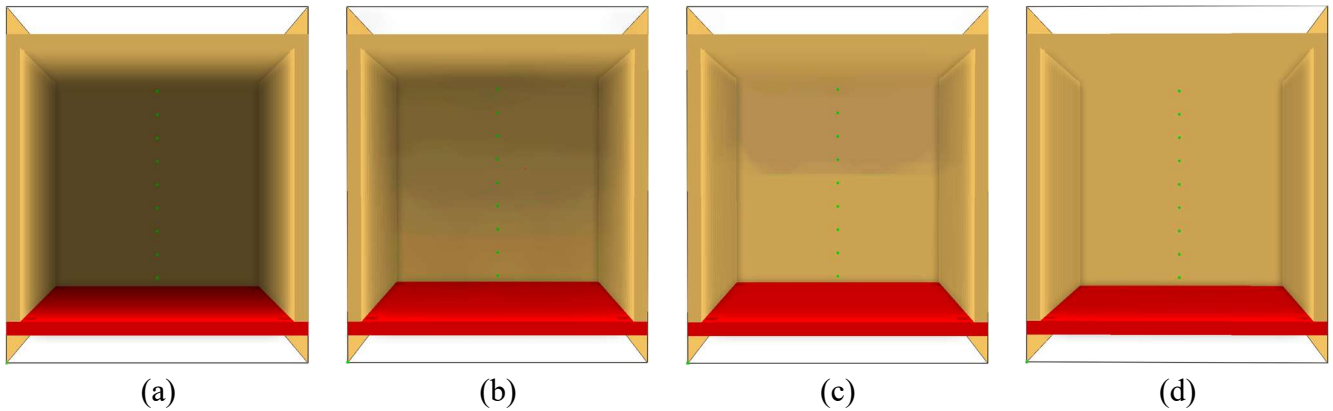


Figure 6. Visualisation of smoke density in Scenario 2 at (a) 0s , (b) 10s, (c) 30s, and (d) 50s.

4.3 Scenario 3

Scenario 3 represents a situation in which no smoke is present anymore. Both the thermocouples and gas inside the compartment are initially at 20°C, representing fresh air that cools the linings inside a compartment after a fire. Immediately after the beginning of the simulation, the air inside the compartment stratifies due to the difference in temperature between the ceiling and the floor, as can be seen in Figure 7b. As they are surrounded by air that is increasing in temperature, the thermocouples follow the same trend, as depicted in Figure 7a. The final temperature of the thermocouples at steady state is, however, higher than the local gas temperature due to influence of radiation, which cannot affect transparent air. The resulting steady-state situation is the same as in Scenarios 1 and 2 as the temperatures of the floor and ceiling are the same.

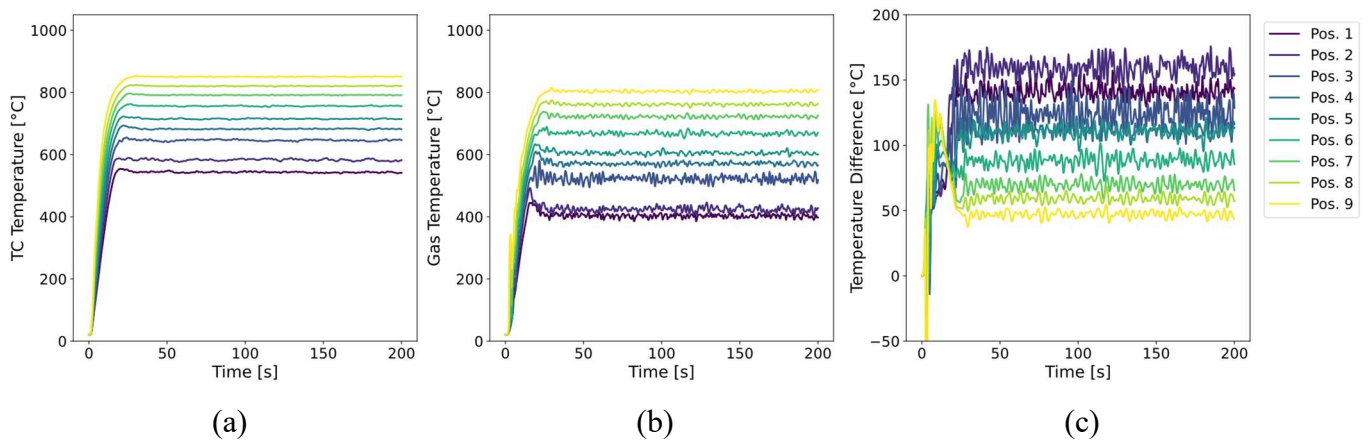


Figure 7. Temperatures measured by (a) thermocouples (TC): T_{TC} and (b) temperature devices (TD): T_g , and (c) the difference $T_{TC} - T_g$ in Scenario 3. Pos. 1 to 9 as specified in Figure 1.

4.4 Sensitivity analysis

To ensure that the chosen cell size does not significantly impact the simulation outcomes, a sensitivity analysis is conducted. Specifically, the configuration from Scenario 2 (5 cm cell size) is compared to results from a simulation utilizing a 2.5 cm cell size in Figure 8. This demonstrates that refining the cell size to 2.5 cm does indeed affect the calculated thermocouple temperatures during the dynamic phase of the simulation, but minimal differences are observed in the steady-state values between the two cell sizes.

Moreover, the observed variation is primarily quantitative and is considered overall acceptable: given that the results are utilized for qualitative analysis purposes, the selected mesh cell size is deemed suitable.

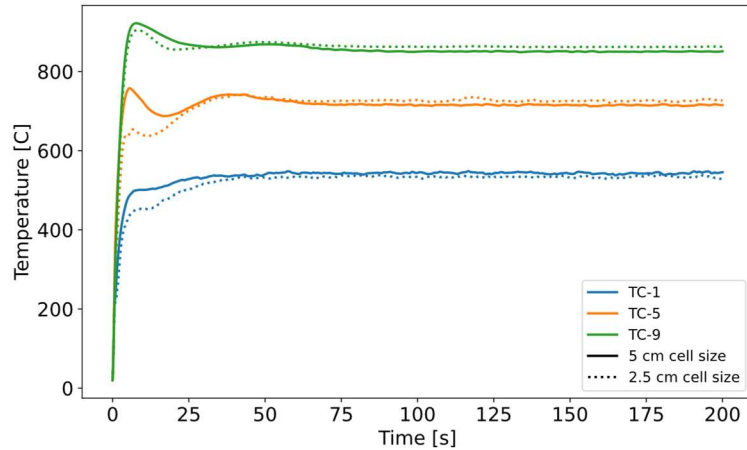


Figure 8. Sensitivity analysis of Scenario 2 employing mesh cell sizes of 5 cm and 2.5 cm.

5 DISCUSSION

The three scenarios presented above demonstrated the difficulties inherent to performing and interpreting temperature measurements in large-scale fire experiments. The temperature measured by a thermocouple is heavily affected by the temperature and optical thickness of smoke, the temperature of the linings and the relative position of the thermocouple to radiating surfaces (usually the linings and the smoke layer). Hence, thermocouples can measure significantly different temperatures depending on where they are located inside a compartment, and depending on the stage of the fire, which influences the environmental conditions governing heat transfer.

The changing conditions during the fire decay and cooling phases have important implications on the use of thermocouple data when applied within the framework of the adiabatic surface temperature, which considers fixed values for the convective heat transfer coefficient, h_{AST} , and the effective emissivity, ϵ_{AST} . These values have been determined for the post-flashover heating and fully-developed phases, but not for the decay and cooling phases. During the post-flashover heating and fully-developed phases, the compartment is often assumed to be filled with a hot, optically thick smoke at uniform temperature, preventing radiative heat transfer between temperature measuring devices and the compartment linings. As the optical thickness of the smoke reduces during the decay phase and the smoke is replaced by fresh and transparent air in the cooling phase, the heat transfer equation becomes more complex as the attenuation coefficient of the smoke, the path length of the radiation through the smoke and temperature differences in the smoke need to be considered. Therefore, thermocouple measurements need to be corrected for radiation coming from the compartment linings, considering the optical thickness of the smoke at every point in space and at every instance of time, similar to the method used in [9].

Applying thermocouple data as an AST, with assumed fixed values for the effective emissivity and convective heat transfer coefficient, is inherently incorrect as the net total heat flux in equation (4) will be different when other values for these parameters are used. It was clearly demonstrated in Scenario 1 that significant differences in the AST can be expected when inappropriate values for the convective heat transfer coefficient and effective emissivity are used. This happens mainly during the decay and cooling phases as the suggested values in literature have been derived for the fully-developed phase. This obstacle can be overcome if their values were adjusted to the thermal boundary conditions in the compartment – a task that is far more complex than it appears at first sight. In particular, the value of the convective heat transfer coefficient should be determined based on the velocity of the gas, the temperature of the gas and the temperature of the thermocouple itself. Nevertheless, this information is generally not, or at least insufficiently detailed, available from large-scale fire experiments. A second option would be to predict

these values using CFD software such as FDS, although there are also differences between simulations and real experiments.

6 CONCLUSIONS

In this study, it was investigated whether thermocouple measurements can be used directly as input for SFE calculations, using the Adiabatic Surface Temperature to define the thermal boundary conditions, in particular during the fire decay and cooling phases. Firstly, the theoretical background of Adiabatic Surface Temperature was revisited to understand the implicit assumptions of the concept. Secondly, a series of canonical FDS simulations, representing the thermal boundary conditions during the decay and cooling phases, were carried out to investigate the influence of the changing smoke and radiation conditions on the temperatures measured by thermocouples.

The results of the FDS simulations indicated that factors such as smoke temperature, smoke's optical thickness, temperature of the linings and thermocouple position have a significant influence on the readings obtained from thermocouples. When an optically thick smoke is present, thermocouples tend to measure the true smoke/gas temperature. These conditions typically occur during the fully-developed phase of a fire. Given the uniformity of conditions and alignment with the convective heat transfer coefficient and effective emissivity used in calculating the Adiabatic Surface Temperature, during this phase thermocouple measurements can effectively be utilized as inputs for Structural Fire Engineering (SFE) calculations.

The thermal boundary conditions however change significantly when the fire transitions into the decay phase and, subsequently, into the cooling phase. Smoke becomes less optically thick due to dilution with fresh air and a decreasing heat release rate. Radiation from compartment linings and other elements will then affect thermocouple measurements. In addition, the fixed values for the convective heat transfer coefficient and effective emissivity are no longer applicable. Hence, thermocouple measurements for the decay and cooling phases cannot directly be used within the framework of the Adiabatic Surface Temperature.

ACKNOWLEDGMENT

This research has been funded by Research Foundation of Flanders (FWO) within the scope of the research project (Grant number 1137123N) "Characterization of the thermal exposure and material properties of concrete during the fire decay phase for performance-based structural fire engineering". Dr. Lucherini would also like to gratefully acknowledge the financial support for the FRISSBE project within the European Union's Horizon 2020 research and innovation program (GA 952395).

REFERENCES

- [1] K. LaMalva and D. Hopkin, Eds., *International Handbook of Structural Fire Engineering*. in The Society of Fire Protection Engineers Series. Cham: Springer International Publishing, 2021. doi: 10.1007/978-3-030-77123-2.
- [2] U. Wickström, *Temperature Calculation in Fire Safety Engineering*. Cham: Springer International Publishing, 2016. doi: 10.1007/978-3-319-30172-3.
- [3] CEN, 'EN 1991-1-2: Eurocode 1: Actions on structures - Part 1-2: general actions - Actions on structures exposed to fire'. European Committee for Standardization, Brussels, Belgium, 2002.
- [4] C. R. Barnett, 'BFD curve: a new empirical model for fire compartment temperatures', *Fire Saf. J.*, vol. 37, no. 5, pp. 437–463, Jul. 2002, doi: 10.1016/S0379-7112(02)00006-1.
- [5] A. Lucherini and J. L. Torero, 'Defining the fire decay and the cooling phase of post-flashover compartment fires', *Fire Saf. J.*, vol. 141, p. 103965, Dec. 2023, doi: 10.1016/j.firesaf.2023.103965.
- [6] Y. A. Cengel, 'Basics of Heat Transfer', in *Heat Transfer: A Practical Approach*, 2nd ed., New York: Mcgraw-Hill, 2002, pp. 1–60.
- [7] K. McGrattan, S. Hostikka, J. Floyd, R. McDermott, M. Vanella, and E. Mueller, 'FDS User's Guide', FDS-SMV. Accessed: Nov. 27, 2023. [Online]. Available: <https://pages.nist.gov/fds-smv/manuals.html>
- [8] Y. A. Cengel, 'Radiation Heat Transfer', in *Heat Transfer: A Practical Approach*, 2nd ed., New York: Mcgraw-Hill, 2002, pp. 605–666.

- [9] S. Welch, A. Jowsey, S. Deeny, R. Morgan, and J. L. Torero, 'BRE large compartment fire tests-Characterising post-flashover fires for model validation', *Fire Saf. J.*, vol. 42, no. 8, pp. 548–567, Nov. 2007, doi: 10.1016/j.firesaf.2007.04.002.